KJO
pISSN: 1011-8942 eISSN: 2092-9382

Korean J Ophthalmol 2024;38(6):496-506
https://doi.org/10.3341/kjo.2024.0115

Original Article

Repeatability of Corneal Epithelial Thickness Map Using Anterior-Segment Optical Coherence Tomography in Normal and Corneal Disease Patients

Jee Eun Lee, Kyung Eun Han

Department of Ophthalmology, Ewha Womans University Mokdong Hospital, Ewha Womans University College of Medicine, Seoul, Korea

Purpose: To evaluate the repeatability of corneal epithelial thickness (CET) measurements in normal eyes and eyes diagnosed with corneal disease using the epithelial thickness map (ETM) of anterior-segment optical coherence tomography (OCT).

Methods: In this retrospective study, patients with three OCT scans using the ETM mode of Cirrus OCT between October 2021 and January 2024 were reviewed. Two groups of subjects were included: (1) normal subjects with no history of ophthalmic surgery, corneal diseases, and topical antiglaucoma medication uses; and (2) subjects with corneal diseases including dry eye syndrome, recurrent corneal erosion, pterygium, and others. A total of 57 eyes of 57 normal subjects and 106 eyes of 76 patients with corneal disease were included. ETM was analyzed in 25 zones (one zone within 0–2 mm diameter, eight zones within 2–5 mm diameter, eight zones within 5–7 mm diameter, and eight zones within 7–9 mm diameter). Repeatability was evaluated by calculating intraclass correlation coefficient (ICC), coefficient of variation (CoV), within-subject standard deviation (Sw), and Bland-Altman plot.

Results: Among a total of 25 sectors, the normal eyes showed high repeatability (ICC, >0.75; CoV, 2.160%–5.292%; Sw, 0.760–1.653 μm) in 23 sectors, and corneal diseases patients also showed high repeatability (ICC, >0.75; CoV, 4.167%–9.606%; Sw, 1.298–3.340 μm) in 22 sectors. However, the wide range of 95% limit of agreement width of Bland-Altman plot presented in corneal disease group and some peripheral zones in normal eyes indicates some variability of CET measurements.

Conclusions: Except for a few peripheral sectors, ETM of Cirrus OCT provides repeatable CET measurements in normal eyes; however in corneal disease group, repeatability was not consistently high. To measure CET accurately, performing multiple measurements is advised especially in patients with corneal disease and patients in whom peripheral CET values.

Key Words: Anterior-segment optical coherence tomography, Corneal epithelial thickness, Corneal topography

Received: September 26, 2024 *Final revision:* October 21, 2024
Accepted: October 21, 2024

Corresponding Author: Kyung Eun Han, MD, PhD. Department of Ophthalmology, Ewha Womans University Mokdong Hospital, Ewha Womans University College of Medicine, 1071 Anyangcheon-ro, Yangcheon-gu, Seoul 07985, Korea. Tel: 82-2-2650-5154, Fax: 82-2654-4334, Email: hanke@ewha.ac.kr

The corneal epithelium plays a crucial role in maintaining optical clarity and visual acuity, providing essential defense and refractive functions [1–3]. Its thickness can change by remodeling process of the corneal epithelium in response to compensation of stromal alterations and is influenced by various factors and pathologic conditions such

as laser refractive surgery, keratoconus (KC), dry eye syndrome, contact lens wear, age, sex, and topical antiglaucoma medication [1–5].

In order to measure corneal epithelial thickness (CET) accurately, high-frequency scanning ultrasound biomicroscopy (HF-UBM), confocal microscopy, and anterior-segment optical coherence tomography (AS-OCT) are used [6]. HF-UBM provides high resolution images unobstructed by optically opaque intervening ocular structures; however, it requires direct contact with the eye, which can be uncomfortable and necessitate greater effort by the examiner and a higher degree of compliance from the patient [7]. Confocal microscopy provides very high axial resolution, but it is unable to provide a holistic view of the cornea to produce topographic mapping with current technology [8].

Topographic mapping of the CET by using OCT was recently developed. OCT makes it possible to measure CET quickly and conveniently without direct contact [4,9–12]. According to previous studies, CET measurements made by using RTVue (OptovueA) topographic mapping and iVue (Optovue) provide high repeatability [13,14]. However, the repeatability of epithelial thickness map (ETM) scans of another the widely used Cirrus OCT (Carl Zeiss Meditec) was not been evaluated. Therefore, the aim of this study is to evaluate the repeatability of CET measurements obtained using the ETM scan of Cirrus OCT in both normal eyes and eyes with corneal disease.

Materials and Methods

Ethics statement

This study was approved by the Institutional Review Board of Ewha Womans University Mokdong Hospital (No. 2024-09-017-001). The requirement for informed consent was waived due to the retrospective nature of the study. The study adhered to the tenets of the Declaration of Helsinki throughout the study.

Subjects

This is a single-center, retrospective, observational study. Patients who visited the hospital and whose CET values were collected using the ETM mode of the Cirrus OCT between October 2021 and January 2024 were reviewed. Two groups of subjects were included: (1) patients with normal eyes; and (2) patients with corneal abnormalities. All patients were 18 years of age or older and were able to complete the required examinations.

Exclusion criteria in the normal group were a history of ocular surgery (laser refractive surgery, cataract surgery, vitrectomy, corneal transplant surgery, etc.), usage of topical antiglaucoma medications, history or current diagnosis of corneal disease, and inability to complete three AS-OCT scans. One eye per individual was included in the normal group. If both eyes qualified, the right eye was selected.

Patients with corneal abnormalities were included if they had a history or current diagnosis of dry eye syndrome, recurrent corneal erosion, pterygium, or another condition. Also, patients with a history of ocular surgery, patients with a history of topical antiglaucoma medication use, and those unable to complete the three AS-OCT scans were

A

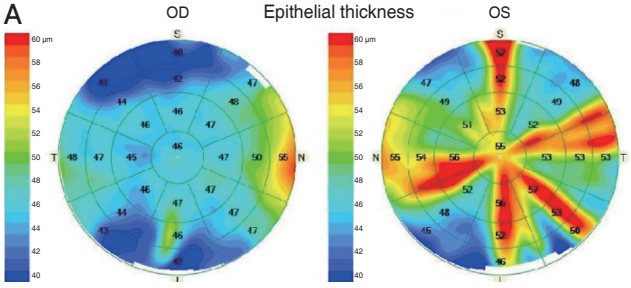

B

Epithelial thickness OD

Range (mm)	Min (μm)	Avg (μm)	Max (μm)	S – I (μm)	SN – IT (μm)
0.0–2.0	44	46	48	-	-
2.0–5.0	43	46	51	–1	1
5.0–7.0	38	46	53	–4	4
7.0–9.0	36	45	60	–2	4

Min thickness (μm)	36	Y min (mm)	–4.3
Min – median (μm)	–3	Central thickness (μm)	47

Epithelial thickness OS

Range (mm)	Min (μm)	Avg (μm)	Max (μm)	S – I (μm)	SN – IT (μm)
0.0–2.0	48	55	62	-	-
2.0–5.0	44	54	65	–3	–6
5.0–7.0	42	51	63	0	–4
7.0–9.0	37	50	69	6	–3

Min thickness (μm)	37	Y min (mm)	–4.3
Min – median (μm)	–10	Central thickness (μm)	56

Fig. 1. Representative epithelial thickness mapping image produced by Cirrus OCT (Carl Zeiss Meditec). (A) Corneal epithelial thickness is shown in 25 sectors (one within 0–2 mm diameter, eight within 2–5 mm diameter, eight within 5–7 mm diameter, and eight within 7–9 mm diameter). (B) Data from analysis software reports. OD = right eye; OS = left eye; S = superior; T = temporal; I = inferior; N = nasal; Min = minimum; Avg = average; Max = maximum.

excluded. In the patient group, if both eyes qualified, then both were included in the study.

Imaging device and measurement technique

CET measurements were conducted using the Cirrus OCT, which utilizes a noninvasive ETM mode. Each eye underwent three consecutive measurements, with a total of 25 corneal zones assessed for repeatability (Fig. 1A, 1B).

For epithelial thickness mapping, the anterior segment module attachment was employed. Patients were positioned with their gaze fixed on a target light, and the imaging was centered on the pupil center. The pachymetry map consisted of eight radial scans (each with 1,024 axial scans) repeated five times, covering an area with a 9 mm diameter. The software algorithm calculated CET as the distance between the middle of the tear film layer and the middle of the anterior surface of the Bowman layer observed on the B scan. Images were captured after aligning the horizontal single scan line with the corneal apex, ensuring the visibility of the hyperreflective corneal reflex. Additional scans were performed if the initial scan was misaligned or showed poor reflection of the corneal apex. Data were exported and analyzed using Cirrus OCT Review Software ver. 11.0 (Carl Zeiss Meditec), which provided average automated measurements of CET for four concentric ring-shaped zones centered on the cornea: central (0–2 mm), paracentral (2–5 mm), mid-peripheral (5–7 mm), and peripheral (7–9 mm). ET data were also presented for specific corneal octants: superior (S), inferior (I), temporal (T), nasal (N), superior nasal (SN), superior temporal (ST), inferior temporal (IT), and inferior nasal (IN) within the paracentral, mid-peripheral, and peripheral zones [15].

Table 1. Corneal disease group diagnosis (n = 106)

Diagnosis	No. of eyes
Dry eye disease	54
Recurrent corneal erosion	26
Pterygium	8
Corneal opacity	5
Superficial punctate keratopathy	3
Corneal neovascularization	2
Filamentary keratitis	2
Corneal abrasion	2
Other	4

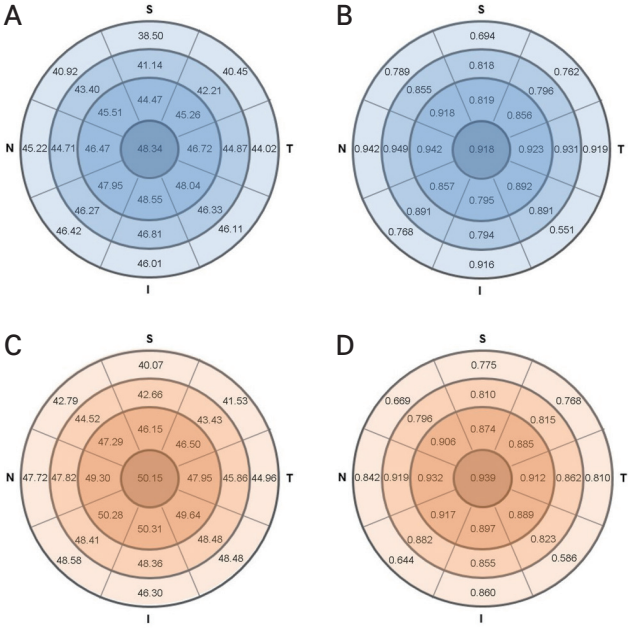

Fig. 2. Corneal epithelial thickness (μm) and intraclass correlation coefficient in (A,B) 57 normal eyes (30 men and 27 men; mean age, 52.6 ± 17.1 years) and (C,D) 106 corneal disease eyes (30 men and 46 women; mean age, 50.1 ± 15.5 years). S = superior; T = temporal; I = inferior; N = nasal.

Table 2. Average of CET, ICC, Sw, CoV, and CR by diameter in normal and corneal disease eyes

Diameter	Normal eye					Corneal disease eye				
	CET (μm)	ICC	Sw (μm)	CoV (%)	CR (μm)	CET (μm)	ICC	Sw (μm)	CoV (%)	CR (μm)
0–2 mm	48.34 ± 3.73	0.918	0.827	2.214	2.941	50.15 ± 7.48	0.939	1.298	5.993	5.076
2–5 mm	46.62 ± 4.23	0.875	1.013	2.973	3.803	48.43 ± 6.89	0.902	1.587	5.816	5.972
5–7 mm	44.47 ± 4.68	0.866	1.136	3.598	4.229	46.19 ± 6.24	0.845	1.767	7.047	6.918
7–9 mm	43.46 ± 5.60	0.793	1.571	4.720	5.775	45.05 ± 6.53	0.744	2.383	9.622	9.097

Values are presented as mean ± standard deviation.
CET = corneal epithelial thickness; ICC = intraclass correlation coefficient; Sw = within-subject standard deviation; CoV = coefficient of variation; CR = coefficient of repeatability.

Statistical analysis

Repeatability was evaluated using the intraclass correlation coefficient (ICC), within-subject standard deviation (Sw), coefficient of variation (CoV), and coefficient of repeatability (CR). The ICC serves as an indicator of the reliability of repeated measurements, and it was calculated using the two-way mixed model and absolute agreement. Its values less than 0.5, 0.5 to less than 0.75, and 0.75 or greater represent poor, moderate, and good repeatability, respectively. To compare ICC value between corneal disease group and normal group, resampling procedure called bootstrap method was used. 1,000 bootstrap samples were generated and 95% coefficient interval (CI) of ICC difference that does not include 0 was considered statistically significant. Sw allows the estimation of variance. The CoV

Table 3. Epithelial thickness repeatability in normal and corneal diseased eyes

Sector	Normal eye			Corneal disease eye			ICC difference	95% CI*
	ICC	Sw (μm)	CoV (%)	ICC	Sw (μm)	CoV (%)		
0–2 mm	0.918	0.827	2.214	0.939	1.298	5.993	0.021	–0.031 to 0.098
2–5 mm								
S	0.819	1.148	3.808	0.874	1.740	6.533	0.055	–0.037 to 0.182
SN	0.918	0.971	2.727	0.906	1.453	5.002	–0.012	–0.066 to 0.069
N	0.942	0.805	2.173	0.932	1.464	4.420	–0.010	–0.047 to 0.046
IN	0.857	1.035	2.947	0.917	1.545	5.502	0.060	–0.019 to 0.220
I	0.795	1.092	3.481	0.897	1.694	6.362	0.102	–0.018 to 0.285
IT	0.892	1.035	2.641	0.889	1.612	7.668	–0.003	–0.101 to 0.093
T	0.923	0.941	2.575	0.912	1.542	5.317	–0.011	–0.056 to 0.054
ST	0.856	1.080	3.431	0.885	1.649	5.721	0.029	–0.052 to 0.160
5–7 mm								
S	0.818	1.369	4.921	0.810	2.043	9.522	–0.008	–0.134 to 0.141
SN	0.855	1.291	4.129	0.796	1.805	6.668	–0.059	–0.158 to 0.069
N	0.949	0.760	2.160	0.919	1.397	4.167	–0.030	–0.073 to 0.014
IN	0.891	1.027	2.928	0.882	1.701	6.027	–0.009	–0.117 to 0.140
I	0.794	1.371	4.223	0.855	1.808	7.306	0.061	–0.087 to 0.236
IT	0.891	1.047	2.853	0.823	1.849	8.439	–0.068	–0.199 to 0.036
T	0.931	0.900	2.589	0.862	1.691	6.308	–0.069	–0.127 to –0.008†
ST	0.796	1.326	4.982	0.815	1.841	7.942	0.019	–0.118 to 0.186
7–9 mm								
S	0.694	1.760	6.695	0.775	1.975	7.765	0.081	–0.146 to 0.285
SN	0.789	1.653	5.134	0.669	2.762	14.120	–0.120	–0.291 to 0.073
N	0.942	0.979	2.821	0.842	1.794	6.392	–0.100	–0.175 to –0.031†
IN	0.768	2.001	5.292	0.644	3.241	11.760	–0.124	–0.252 to 0.115
I	0.916	1.239	3.262	0.860	2.077	6.427	–0.056	–0.157 to 0.012
IT	0.551	2.283	6.406	0.586	3.340	13.360	0.035	–0.266 to 0.258
T	0.919	1.017	3.005	0.810	1.869	7.553	–0.109	–0.189 to –0.016†
ST	0.762	1.632	5.148	0.768	2.009	9.606	0.006	–0.180 to 0.232

ICC = intraclass correlation coefficient; CI = confidence interval; Sw = within-subject standard deviation; CoV = coefficient of variation; S = superior; SN = superior nasal; N = nasal; IN = inferior nasal; I = inferior; IT = inferior temporal; T = temporal; ST = superior temporal.
*The 95% CI of ICC difference was obtained from 1,000 resampling by bootstrap methods; †The 95% CI that does not include 0, was considered as statistically significant.

was calculated as the Sw divided by the mean of the measurements (CoV = Sw / mean × 100%). The CoV allows a comparison between data that have different means. A larger CoV reflects a greater level of dispersion around the mean. Bland-Altman plots were used to analysis the distribution of variability by size, mean difference and 95% limit of agreement (LoA), and CR of three pairs, which were formed by combining two out of the three measurements: pair 1 (measurement 1 – measurement 2), pair 2 (measurement 2 – measurement 3), and pair 3 (measurement 3 – measurement 1). All statistical analyses were performed using IBM SPSS ver. 26.0 (IBM Corp), R ver. 4.4.1 (R Core Team), and MedCalc ver. 23.0.5 (MedCalc Software).

Results

The normal group consisted of 57 eyes of 57 patients (30 men and 27 women) with a mean age of 52.6 ± 17.1 years, while the corneal disease group included 106 eyes of 76 patients (30 men and 46 women), with a mean age of 50.1 ± 15.5 years. Enrolled subjects with corneal pathology had one of the diagnoses listed in Table 1.

The average CET and repeatability factor by diameter in normal and corneal disease eyes are presented in Table 2. In the normal eyes group, the average CET for the 0–2 mm diameter zone was 48.34 ± 3.73 μm, with an ICC of 0.918, Sw of 0.827 μm, CoV of 2.214%, and CR of 2.941 μm. For the 2–5 mm diameter zone, the average CET was 46.62 ± 4.23 μm, ICC was 0.875, Sw was 1.013 μm, CoV was 2.973%, and CR was 3.803 μm. In the 5–7 mm zone, the average CET was 44.47 ± 4.68 μm, ICC was 0.866, Sw was 1.136 μm, CoV was 3.598%, and CR was 4.229 μm. Finally, in the peripheral 7–9 mm zone, the average CET was 43.46 ± 5.60 μm, ICC was 0.793, Sw was 1.571 μm, CoV was 4.720%, and CR was 5.775 μm. For the corneal disease group, the average CET in the 0–2 mm diameter zone was 50.15 ± 7.48 μm, with an ICC of 0.939, Sw of 1.298 μm, CoV of 5.993%, and CR of 5.076 μm. In the 2–5 mm zone, the average CET was 48.43 ± 6.89 μm, ICC was 0.902, Sw was 1.587 μm, CoV was 5.816%, and CR was 5.972 μm. For the 5–7 mm zone, the average CET was 46.19 ± 6.24 μm, ICC was 0.845, Sw was 1.767 μm, CoV was 7.047%, and CR was 6.918 μm. In the 7–9 mm zone, the average CET was 45.05 ± 6.53 μm, ICC was 0.744, Sw was 2.383 μm, CoV was 9.622%, and CR was 9.097 μm.

Fig. 2A–2D and Table 3 shows CET and repeatability in-

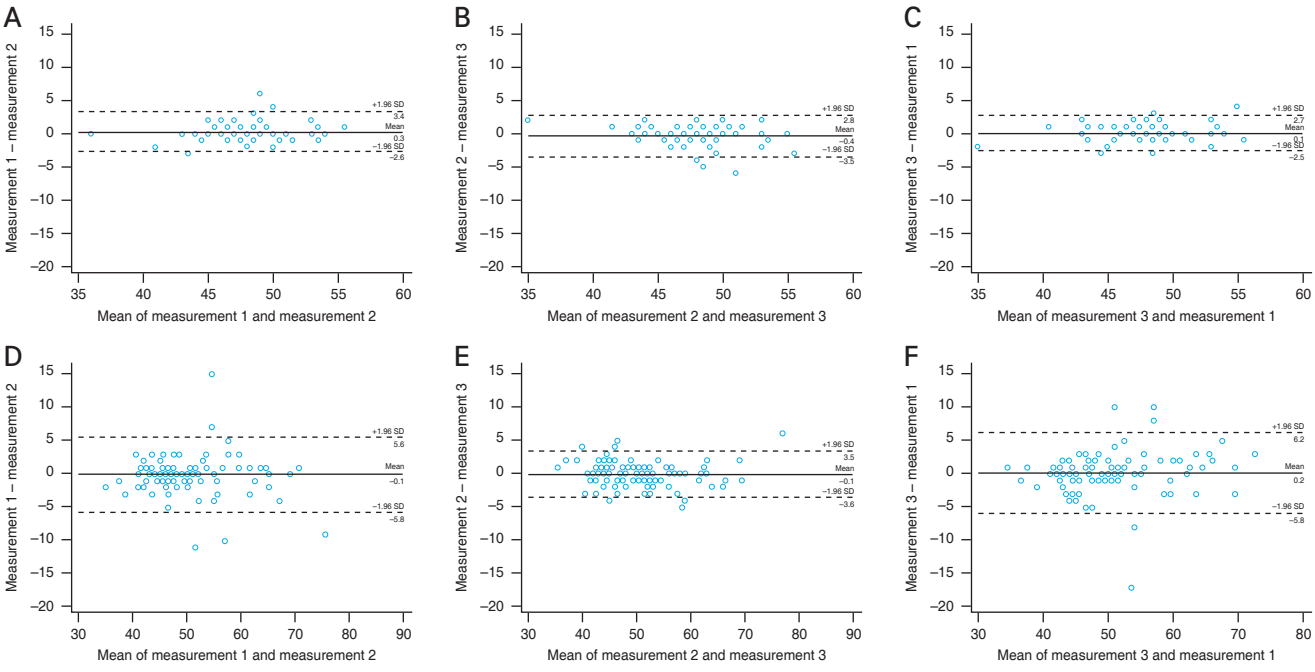

Fig. 3. Representative figure of Bland-Altman Plots of three pairs at 0–2 mm zone in (A–C) normal eyes and (D–F) corneal disease eyes. (A,D) Pair 1 (measurement 1 – measurement 2). (B,E) Pair 2 (measurement 2 – measurement 3). (C,F) Pair 3 (measurement 3 – measurement 1). SD = standard deviation.

dex by sectors of normal and corneal disease patients. Out of 25 sectors, the normal eyes showed high repeatability (ICC, >0.75; CoV, 2.160%–5.292%; Sw, 0.760–1.653 μm) in 23 sectors except for 2 sectors (7–9 mm S and IT), and patients with corneal diseases also showed high repeatability (ICC, >0.75; CoV, 4.167%–9.606%; Sw, 1.298–3.340 μm) in 22 sectors, except for 3 sectors (7–9 mm SN, IN, and IT). The 95% CI of the ICC difference between two groups, calculated after 1,000 of resampling using the bootstrap method, is also presented in Table 3. There was no statistically significant difference between ICC values of normal and corneal disease groups, except in three sectors, 5–7 mm T, 7–9 mm N, and 7–9 mm T, although these three zones are neither significant regions nor regions with low repeatability indicators.

Fig. 3A–3F and Supplementary Fig. 1–3 show Bland-Altman plots of three pairs at every sector in normal and corneal disease patients. Tables 4 and 5 present the repeatabil-

Table 4. Mean difference, 95% LoA, and CR analyzed using the Bland-Altman plot in normal eyes

Sector	Mean difference (μm)			95% LoA (μm)			CR (μm)		
	Pair 1	Pair 2	Pair 3	Pair 1	Pair 2	Pair 3	Pair 1	Pair 2	Pair 3
0–2 mm	0.28	–0.37	0.09	–2.813 to 3.374	–3.525 to 2.788	–2.486 to 2.662	3.094	3.157	2.574
2–5 mm									
S	0.09	–0.02	–0.07	–4.660 to 4.835	–4.361 to 4.326	–4.855 to 4.715	4.748	4.343	4.785
SN	0.00	–0.33	0.33	–3.572 to 3.572	–3.527 to 2.860	–3.028 to 3.694	3.572	3.194	3.361
N	0.16	–0.25	0.09	–2.777 to 3.093	–2.626 to 2.134	–2.928 to 3.103	2.935	2.380	3.016
IN	0.00	–0.12	0.12	–3.741 to 3.741	–3.991 to 3.746	–3.936 to 4.182	3.741	3.868	4.059
I	0.37	–0.02	–0.35	–5.354 to 6.090	–3.462 to 3.427	–4.834 to 4.132	5.722	3.445	4.483
IT	0.04	0.02	–0.05	–3.193 to 3.264	–4.148 to 4.183	–3.354 to 3.248	3.228	4.166	3.301
T	0.37	–0.21	–0.16	–2.999 to 3.736	–3.518 to 3.097	–3.467 to 3.151	3.367	3.308	3.309
ST	0.19	–0.58	0.39	–4.945 to 5.331	–5.038 to 3.881	–2.963 to 3.735	5.138	4.459	3.349
5–7 mm									
S	–0.16	0.00	0.09	–6.334 to 6.012	–3.832 to 3.832	–5.788 to 5.967	6.173	3.832	5.877
SN	0.19	–0.05	–0.14	–4.727 to 5.113	–5.069 to 4.964	–4.684 to 4.403	4.920	5.017	4.543
N	0.28	–0.28	0.00	–2.460 to 3.022	–2.557 to 1.995	–2.869 to 2.869	2.741	2.276	2.869
IN	0.16	–0.28	0.12	–3.561 to 3.877	–3.483 to 2.922	–4.245 to 4.491	3.719	3.203	4.368
I	0.49	–0.32	–0.25	–5.763 to 6.746	–3.770 to 3.127	–5.708 to 5.208	6.255	3.448	5.458
IT	0.02	–0.02	0.00	–3.805 to 3.840	–4.200 to 4.165	–3.229 to 3.229	3.822	4.182	3.229
T	0.39	–0.37	–0.02	–2.752 to 3.524	–3.205 to 2.468	–3.32 to 3.285	3.138	2.836	3.302
ST	0.67	–0.96	0.30	–5.229 to 6.562	–6.370 to 4.441	–4.685 to 5.281	5.896	5.405	4.983
7–9 mm									
S	–0.12	0.17	–0.15	–9.181 to 8.943	–5.542 to 5.883	–6.757 to 6.457	9.062	5.713	6.607
SN	–0.36	–0.23	0.44	–5.957 to 5.237	–6.412 to 5.950	–5.364 to 6.239	5.597	6.181	5.802
N	0.46	–0.19	–0.26	–2.555 to 3.467	–3.536 to 3.150	–3.826 to 3.300	3.011	3.343	3.563
IN	0.13	–0.20	–0.04	–7.946 to 8.200	–7.442 to 7.034	–5.489 to 5.416	8.073	7.238	5.453
I	0.00	0.00	–0.14	–3.851 to 3.851	–3.719 to 3.719	–5.202 to 4.929	3.851	3.719	5.065
IT	–0.34	0.58	–0.26	–11.800 to 11.121	–10.452 to 11.622	–5.766 to 5.248	11.461	11.037	5.507
T	0.50	–0.14	–0.30	–2.780 to 3.780	–3.516 to 3.230	–4.321 to 3.725	3.280	3.373	4.023
ST	0.52	–0.15	–0.32	–6.198 to 7.236	–4.833 to 4.537	–6.564 to 5.922	6.717	4.685	6.243

Pair 1, "measurement 1 – measurement 2"; pair 2, "measurement 2 – measurement 3"; and pair 3, "measurement 3 – measurement 1". LoA = limit of agreement; CR = coefficient of repeatability; S = superior; SN = superior nasal; N = nasal; IN = inferior nasal; I = inferior; IT = inferior temporal; T = temporal; ST = superior temporal.

ity metrics analyzed using the Bland-Altman plot in normal and corneal disease patients. For the normal group, the mean difference ranged from –0.96 to 0.67 μm, 95% LoA width ranged from 4.552 to 22.074 μm, and the CR ranged from 2.276 to 11.461 μm. For the corneal disease group, the mean difference ranged from –0.90 to 0.78 μm, 95% LoA width ranged from 7.080 to 27.438 μm, and the CR ranged from 3.540 to 13.719 μm. In both normal and corneal disease groups, the absolute value of the mean difference was less than 1 μm, however, wide 95% LoA range were found in corneal disease eyes and peripheral zones in both groups.

Overall, ICC values in both groups indicated high repeatability in the central to mid-peripheral zones (0–2, 2–5, and 5–7 mm), while peripheral zones (7–9 mm) showed reduced reliability, particularly in the corneal disease group. Sw, CoV, and CR values show increasing trends toward the periphery, indicating greater variability in these regions.

Table 5. Mean difference, 95% LoA, and CR analyzed using the Bland-Altman plot in corneal disease eyes

Sector	Mean difference (μm)			95% LoA (μm)			CR (μm)		
	Pair 1	Pair 2	Pair 3	Pair 1	Pair 2	Pair 3	Pair 1	Pair 2	Pair 3
0-2 mm	–0.10	–0.07	0.17	–5.778 to 5.570	–3.606 to 3.474	–5.845 to 6.185	5.674	3.540	6.015
2–5 mm									
S	0.22	–0.35	0.13	–6.207 to 6.641	–5.678 to 4.980	–6.433 to 6.698	6.424	5.329	6.565
SN	–0.08	–0.14	0.23	–5.442 to 5.272	–5.306 to 5.023	–4.880 to 5.332	5.357	5.164	5.106
N	–0.18	–0.01	0.19	–5.317 to 4.959	–5.543 to 5.524	–4.880 to 5.257	5.138	5.534	5.069
IN	–0.21	–0.31	0.52	–5.716 to 5.301	–6.246 to 5.624	–5.774 to 6.812	5.509	5.935	6.293
I	0.09	–0.21	0.11	–6.687 to 6.876	–6.474 to 6.059	–6.906 to 7.132	6.782	6.267	7.019
IT	0.26	–0.03	–0.24	–7.436 to 7.964	–5.078 to 5.021	–7.808 to 7.336	7.700	5.050	7.572
T	–0.25	–0.12	0.37	–6.553 to 6.063	–5.289 to 5.043	–5.474 to 6.209	6.308	5.166	5.841
ST	0.07	–0.21	0.14	–6.169 to 6.301	–6.358 to 5.939	–5.670 to 5.956	6.235	6.148	5.813
5–7 mm									
S	–0.09	–0.03	–0.23	–7.263 to 7.093	–7.400 to 7.338	–7.509 to 7.057	7.178	7.369	7.283
SN	0.01	0.20	–0.23	–6.750 to 6.769	–5.892 to 6.292	–6.877 to 6.420	6.759	6.092	6.648
N	–0.02	–0.22	0.24	–5.395 to 5.357	–5.124 to 4.690	–4.415 to 4.886	5.376	4.907	4.650
IN	–0.24	–0.15	0.39	–7.562 to 7.091	–6.348 to 6.046	–7.975 to 8.749	7.326	6.197	8.362
I	0.36	–0.27	0.02	–7.011 to 7.737	–7.778 to 7.229	–7.462 to 7.500	7.374	7.504	7.481
IT	0.06	0.21	–0.23	–9.087 to 9.201	–7.126 to 7.549	–8.163 to 7.706	9.144	7.337	7.935
T	–0.07	–0.03	0.09	–7.116 to 6.984	–6.398 to 6.341	–7.142 to 7.330	7.050	6.370	7.236
ST	–0.08	–0.52	0.44	–6.443 to 6.291	–7.530 to 6.492	–6.650 to 7.523	6.367	7.011	7.086
7–9 mm									
S	0.32	0.13	0.28	–7.428 to 8.072	–6.281 to 6.531	–7.803 to 8.369	7.750	6.406	8.086
SN	–0.02	0.24	–0.56	–8.111 to 8.063	–8.796 to 9.284	–13.453 to 12.331	8.087	9.040	12.892
N	–0.27	0.01	0.31	–8.202 to 7.668	–5.992 to 6.011	–6.317 to 6.939	7.935	6.001	6.628
IN	0.16	–0.13	–0.13	–11.488 to 11.818	–11.994 to 11.726	–12.810 to 12.542	11.653	11.860	12.676
I	–0.10	–0.39	0.49	–9.097 to 8.904	–8.319 to 7.539	–6.043 to 7.030	9.001	7.929	6.536
IT	–0.44	0.45	–0.08	–14.158 to 13.280	–12.654 to 13.560	–13.753 to 13.584	13.719	13.107	13.668
T	0.14	0.01	–0.19	–7.926 to 8.209	–6.420 to 6.439	–8.101 to 7.720	8.067	6.429	7.911
ST	–0.90	0.78	0.17	–9.031 to 7.236	–7.690 to 9.248	–6.177 to 6.518	8.133	8.469	6.347

Pair 1, "measurement 1 – measurement 2"; pair 2, "measurement 2 – measurement 3"; and pair 3, "measurement 3 – measurement 1". LoA = limit of agreement; CR = coefficient of repeatability; S = superior; SN = superior nasal; N = nasal; IN = inferior nasal; I = inferior; IT = inferior temporal; T = temporal; ST = superior temporal.

This variability was more pronounced in the corneal disease group, where CoV exceeded 9% in the 7–9 mm zone, suggesting less consistent measurements and greater individual variation compared to the normal eyes group. In both groups, repeatability and measurement rate showed a decreasing trend as the diameter increased. The measurement rate was nearly 100% for diameters up to 7 mm, but the average measurement rate for the 7–9 mm diameter was 93% (ranging from 81% to 100%) in the normal eyes group and 88% (ranging from 66% to 100%) in the corneal disease group.

Discussion

The aim of this study was to determine the repeatability of CET measurements with the ETM of AS-OCT (Cirrus OCT) in normal and diseased corneas. We evaluated repeatability using various methods, including ICC, Sw, CoV, and Bland-Altman plot. Even though good repeatability was observed in both groups except for some peripheral zones between 7 and 9 mm in ICC, CoV, and Sw values, wide range of 95% LoA of Bland-Altman plot indicated considerable variability in the corneal disease group. Furthermore, both the normal and corneal disease groups exhibited a decreasing trend in repeatability metrics and measurement rates as the diameter extended toward the periphery.

Several previous studies have evaluated the repeatability of ETM using AS-OCT in normal eyes by measuring key statistical parameters (ICC, Sw, and CoV), which provide objective measures of the consistency and reliability of ETM measurements across different devices and ocular conditions. Kanellopoulos and Asimellis [16] used RTVue SD-OCT, which employs a scan of 17 sectors (one sector for 0–2 mm, eight sectors for 2–5 mm, and eight sectors for 5–6 mm), with 373 normal subjects and reported Sw 0.88 ± 0.71 μm in the center. Hashmani et al. [17] used wide 25 sectors, 9-mm Optovue SD-OCT with 220 normal subjects, and they reported ICCs of 0.703 to 0.812 at the inner circle, 0.712 to 0.917 at the middle circle, and 0.796 to 0.930 at the outer circle, which indicates good repeatability in most zones except a few sectors (center, inner IN, I, IT, and middle IN), and there was no significant difference between the repeatability of the center, paracentral, and periphery. Sikorski [18] used REVO NX (Optopol Technology), 17 sectors with 7-mm diameter, on 137 patients with normal eyes, and the ICC was 0.95 at the center (0–2 mm), 0.82 to 0.91 at paracentral (2–5 mm), and 0.64 to 0.89 at peripheral (5–7 mm); they noted high repeatability in most areas except for some at the periphery (5–7 mm S, T, IT, SN), and the repeatability value diminished toward the periphery. Sella et al. [4] reported good corneal ETM repeatability (standard deviation: 0.9 μm at 0–2 mm, 0.9–1.3 μm at 2–5 mm, 1.0–1.4 μm at 5–6 mm), and values decreased toward peripheral in 12 normal eyes across all zones with iVue, which provides scans of 17 sectors (one sector for 0–2 mm, eight sectors for 2–5 mm, and eight sectors for 5–6 mm). Similar to the above studies, except for one study by Hashmani et al. [17] that reported no significant difference between the center and the periphery, our study also showed that repeatability values tend to decrease towards the periphery in all repeatability indices including ICC, Sw, CoV, and CR values. Reinstein et al. [19] suggested that the reason for the decline in the signal quality of CET measurements taken further from the center is that as measurements shift toward the periphery, the OCT beam fails to strike the cornea at optimal angles, resulting in diminished reflection and inadequate signal production.

It is essential to understand normal values and variation patterns in CET for interpreting the information provided by ETM, which has extensive clinical applications by enhancing diagnosis and management of corneal disorders like KC, corneal dystrophies, limbal stem cell deficiency, and dry eye disease [20,21]. Furthermore, the ETM improves refractive surgery safety and efficacy through better patient screening, procedure planning, and postoperative monitoring [21,22]. Analysis of ETM data and pattern alterations may help diagnosing and staging of KC and evaluating the efficacy of collagen crosslinking and combined procedures [23,24].

Previous studies have evaluated the repeatability of CET measurements using the ETM of AS-OCT in patients with corneal diseases, and most were conducted using RTVue—except for one by Li et al. [25]. Ma et al. [13] reported good repeatability with an ICC of 0.891 or higher in all regions for 45 post–laser-assisted *in situ* keratomileusis (post-LASIK) eyes. Mohr et al. [26] reported good repeatability with an ICC ranging from 0.841 to 0.981 in all regions for 59 KC eyes and also observed a trend toward reduced repeatability value with increased distance from the center. Lu et al. [27] investigated 68 post–photorefractive

keratectomy eyes (CoV, 2.6%–6.2%), 61 post–small incision lenticule extraction (post-SMILE) eyes (CoV, 2.3%–4.7%), 75 post–femtosecond LASIK eyes (CoV, 4.0%–6.3%), 20 mild KC eyes (CoV, 2.5%–6.2%), and 53 advanced KC eyes (CoV, 3.5%–8.0%); CoV values were higher in advanced KC compared to mild KC patients. Li et al. [25] used REVO NX, which employs a scan of nine sectors (center, S, ST, T, IT, I, IN, N, SN) at 8-mm diameter, with 259 KC eyes and reported good repeatability in all sectors (ICC, 0.82–0.95; CoV, 3.20%–5.46%). Consistent with the previous studies, the present study also showed good repeatability indices of CET measurements using ETM in patients with corneal diseases in 22 sectors, ICC of 0.768 to 0.939, CoV of 4.17% to 9.61%, and Sw of 1.29 to 3.34 μm, except for 7–9 mm sectors of SN (ICC, 0.669; CoV, 14.12%; Sw, 2.762 μm), IN (ICC, 0.644; CoV, 11.76%; Sw, 3.241 μm), and IT (ICC, 0.586; CoV, 13.36%; Sw, 3.340 μm). Moreover, there was no statistically significant difference between two groups when comparing the ICC values using the bootstrap method. However, the wide 95% LoA width of Bland-Altman plot in all zones in corneal disease showed considerable reliability in these patients. Further investigation involving large cohort of patients with various corneal disease is needed to achieve consistent repeatability indices and conclude the repeatability of CET measurements with ETM of Cirrus OCT in corneal disease patients.

The average center CET of the normal group in this study was 48.3 ± 3.7 μm, similar to a study by Loureiro et al. [20] that reported center CET in 20 normal eye measurements by using Cirrus OCT to be 47.9 ± 1.2 μm. Unlike the results using Cirrus OCT, center CET measurements of normal subjects using RTVue reported in other studies are 52.8 ± 3.6 μm [5], 53.3 ± 3.3 μm [16], 52.3 ± 3.6 μm [28], and 50.5 ± 3.9 μm [29]. When comparing the center CET measurements of Cirrus OCT with RTVue center CET value, OCT with Cirrus was approximately 4 to 5 μm smaller than in RTVue devices, which is in agreement with Loureiro et al. [20]. The Cirrus OCT measures CET as the distance from the midpoint of the tear film to the midpoint of the anterior surface of the Bowman layer, which excludes some portion of the tear film [15]. In contrast, RTVue and iVue include the tear film in their measurements. Tear film is known to be about 2 to 5.5 μm [21,23,30], and since this value is similar to the difference in thickness seen in studies, this CET measurement difference can be estimated by including the tear film layer in OCT measurement.

In conclusion, Cirrus OCT ETM can be used reliably for CET measurement in normal eyes, but in corneal disease eyes, repeatability indices were not consistently high, making it advisable to perform multiple measurements to confirm the CET values. The observed variability in peripheral zones is consistent with previous studies using other OCT devices, suggesting inherent challenges in measuring these areas. This study offers foundational data for accurate CET assessment. The high repeatability in central zones underscores the potential of the Cirrus OCT as a valuable tool in clinical settings for diagnosing and monitoring corneal health. Further studies could explore strategies to enhance measurement reliability in peripheral regions.

Conflicts of Interest: None.
Acknowledgements: None.
Funding: None.

Supplementary Materials

Supplementary Fig. 1. Bland-Altman plots of three pairs in each sector of 2–5 mm diameter in normal and corneal disease eyes.
Supplementary Fig. 2. Bland-Altman plots of three pairs in each sector of 5–7 mm diameter in normal and corneal disease eyes.
Supplementary Fig. 3. Bland-Altman plots of three pairs in each sector of 7–9 mm diameter in normal and corneal disease eyes.

Supplementary materials are available from https://doi.org/10.3341/kjo.2024.0115.

References

1. Samy MM, Shaaban YM, Badran TA. Age- and sex-related differences in corneal epithelial thickness measured with spectral domain anterior segment optical coherence tomography among Egyptians. *Medicine (Baltimore)* 2017; 96:e8314.
2. Kim BJ, Ryu IH, Kim SW. Age-related differences in corneal epithelial thickness measurements with anterior seg-

ment optical coherence tomography. *Jpn J Ophthalmol* 2016;60:357–64.
3. Yang Y, Hong J, Deng SX, Xu J. Age-related changes in human corneal epithelial thickness measured with anterior segment optical coherence tomography. *Invest Ophthalmol Vis Sci* 2014;55:5032–8.
4. Sella R, Zangwill LM, Weinreb RN, Afshari NA. Repeatability and reproducibility of corneal epithelial thickness mapping with spectral-domain optical coherence tomography in normal and diseased cornea eyes. *Am J Ophthalmol* 2019;197:88–97.
5. Nam M, Kim SW. Changes in corneal epithelial thickness induced by topical antiglaucoma medications. *J Clin Med* 2021;10:3464.
6. Kanellopoulos AJ, Asimellis G. In vivo 3-dimensional corneal epithelial thickness mapping as an indicator of dry eye: preliminary clinical assessment. *Am J Ophthalmol* 2014;157:63–68.
7. Kanellopoulos AJ, Aslanides IM, Asimellis G. Correlation between epithelial thickness in normal corneas, untreated ectatic corneas, and ectatic corneas previously treated with CXL; is overall epithelial thickness a very early ectasia prognostic factor? *Clin Ophthalmol* 2012;6:789–800.
8. Le Q, Chen Y, Yang Y, Xu J. Measurement of corneal and limbal epithelial thickness by anterior segment optical coherence tomography and in vivo confocal microscopy. *BMC Ophthalmol* 2016;16:163.
9. Kanellopoulos AJ, Asimellis G. Comparison of high-resolution Scheimpflug and high-frequency ultrasound biomicroscopy to anterior-segment OCT corneal thickness measurements. *Clin Ophthalmol* 2013;7:2239–47.
10. Kanellopoulos AJ, Asimellis G. Anterior segment optical coherence tomography: assisted topographic corneal epithelial thickness distribution imaging of a keratoconus patient. *Case Rep Ophthalmol* 2013;4:74–8.
11. Feng Y, Reinstein DZ, Nitter T, et al. Epithelial thickness mapping in keratoconic corneas: repeatability and agreement between CSO MS-39, Heidelberg Anterion, and Optovue Avanti OCT devices. *J Refract Surg* 2023;39:474–80.
12. Levy A, Georgeon C, Knoeri J, et al. Corneal epithelial thickness mapping in the diagnosis of ocular surface disorders involving the corneal epithelium: a comparative study. *Cornea* 2022;41:1353–61.
13. Ma XJ, Wang L, Koch DD. Repeatability of corneal epithelial thickness measurements using Fourier-domain optical coherence tomography in normal and post-LASIK eyes. *Cornea* 2013;32:1544–8.
14. Hashmani N, Hashmani S, Saad CM. Wide corneal epithelial mapping using an optical coherence tomography. *Invest Ophthalmol Vis Sci* 2018;59:1652–8.
15. Salman A, Mazzotta C, Kailani O, et al. Diagnostic accuracy of corneal and epithelial thickness map parameters to detect keratoconus and suspect keratoconus. *J Ophthalmol* 2023;2023:6677932.
16. Kanellopoulos AJ, Asimellis G. In vivo three-dimensional corneal epithelium imaging in normal eyes by anterior-segment optical coherence tomography: a clinical reference study. *Cornea* 2013;32:1493–8.
17. Hashmani N, Hashmani M, Hashmani S, et al. The influence of tomographic corneal characteristics on epithelial thickness profile. *Cureus* 2020;12:e11731.
18. Sikorski BL. Simultaneous corneal topography and epithelial thickness mapping from a single measurement using optical coherence tomography. *J Ophthalmol* 2022;2022:7339306.
19. Reinstein DZ, Yap TE, Archer TJ, et al. Comparison of corneal epithelial thickness measurement between Fourier-domain OCT and very high-frequency digital ultrasound. *J Refract Surg* 2015;31:438–45.
20. Loureiro T, Rodrigues-Barros S, Carreira AR, et al. Corneal epithelial thickness changes after topical treatment of dry eye disease in primary Sjogren syndrome. *Clin Ophthalmol* 2023;17:993–1005.
21. Abtahi MA, Beheshtnejad AH, Latifi G, et al. Corneal epithelial thickness mapping: a major review. *J Ophthalmol* 2024;2024:6674747.
22. Asroui L, Dupps WJ Jr, Randleman JB. Determining the utility of epithelial thickness mapping in refractive surgery evaluations. *Am J Ophthalmol* 2022;240:125–34.
23. Lin K, Xu Z, Wang H, et al. Comparison of the repeatability and reproducibility of corneal thickness mapping using optical coherence tomography according to tear film breakup time. *BMC Ophthalmol* 2024;24:275.
24. Vega-Estrada A, Mimouni M, Espla E, et al. Corneal epithelial thickness intrasubject repeatability and its relation with visual limitation in keratoconus. *Am J Ophthalmol* 2019;200:255–62.
25. Li Y, Gokul A, McGhee C, Ziaei M. Repeatability of corneal and epithelial thickness measurements with anterior segment optical coherence tomography in keratoconus. *PLoS One* 2021;16:e0248350.
26. Mohr N, Shajari M, Krause D, et al. Pellucid marginal de-

generation versus keratoconus: distinction with wide-field SD-OCT corneal sublayer pachymetry. *Br J Ophthalmol* 2021;105:1638–44.
27. Lu NJ, Chen D, Cui LL, et al. Repeatability of cornea and sublayer thickness measurements using optical coherence tomography in corneas of anomalous refractive status. *J Refract Surg* 2019;35:600–5.
28. Li Y, Tan O, Brass R, et al. Corneal epithelial thickness mapping by Fourier-domain optical coherence tomography in normal and keratoconic eyes. *Ophthalmology* 2012;119:2425–33.
29. Rocha KM, Perez-Straziota CE, Stulting RD, Randleman JB. SD-OCT analysis of regional epithelial thickness profiles in keratoconus, postoperative corneal ectasia, and normal eyes. *J Refract Surg* 2013;29:173–9.
30. Garhofer G, Dos Santos VA, Stegmann H, et al. The association between tear film thickness as measured with OCT and symptoms and signs of dry eye disease: a pooled analysis of 6 clinical trials. *J Clin Med* 2020;9:3791.

Supplementary Fig. 1. Bland-Altman plots of three pairs in each sector of 2–5 mm diameter in normal and corneal disease eyes. Normal eyes: (A1–A3) superior (S); (B1–B3) superior nasal (SN); (C1–C3) nasal (N); (D1–D3) inferior nasal (IN); (E1–E3) inferior (I); (F1–F3) inferior temporal (IT); (G1–G3) temporal (T); and (H1–H3) superior temporal (ST). Corneal disease eyes: (I1–I3) S; (J1–J3) SN; (K1–K3) N; (L1–L3) IN; (M1–M3) I; (N1–N3) IT; (O1–O3) T; and (P1–P3) ST. The mean difference (continuous line), lower and upper 95% limits of agreement (peripheral dotted lines) are depicted.

Supplementary Fig. 2. Bland-Altman plots of three pairs in each sector of 5–7 mm diameter in normal and corneal disease eyes. Normal eyes: (A1–A3) superior (S); (B1–B3) superior nasal (SN); (C1–C3) nasal (N); (D1–D3) inferior nasal (IN); (E1–E3) inferior (I); (F1–F3) inferior temporal (IT); (G1–G3) temporal (T); and (H1–H3) superior temporal (ST). Corneal disease eyes: (I1–I3) S; (J1–J3) SN; (K1–K3) N; (L1–L3) IN; (M1–M3) I; (N1–N3) IT; (O1–O3) T; and (P1–P3) ST. The mean difference (continuous line), lower and upper 95% limits of agreement (peripheral dotted lines) are depicted.

Supplementary Fig. 3. Bland-Altman plots of three pairs in each sector of 7–9 mm diameter in normal and corneal disease eyes. Normal eyes: (A1–A3) superior (S); (B1–B3) superior nasal (SN); (C1–C3) nasal (N); (D1–D3) inferior nasal (IN); (E1–E3) inferior (I); (F1–F3) inferior temporal (IT); (G1–G3) temporal (T); and (H1–H3) superior temporal (ST). Corneal disease eyes: (I1–I3) S; (J1–J3) SN; (K1–K3) N; (L1–L3) IN; (M1–M3) I; (N1–N3) IT; (O1–O3) T; and (P1–P3) ST. The mean difference (continuous line), lower and upper 95% limits of agreement (peripheral dotted lines) are depicted.